

HyperSeed: Unsupervised Learning with Vector Symbolic Architectures

Evgeny Osipov, Sachin Kahawala, Dilantha Haputhanthri, Thimal Kempitiya, Daswin De Silva, Damminda Alahakoon, Denis Kleyko

Abstract—Motivated by recent innovations in biologically-inspired neuromorphic hardware, this paper presents a novel unsupervised machine learning approach named Hyperseed that leverages Vector Symbolic Architectures (VSA) for fast learning a topology preserving feature map of unlabelled data. It relies on two major capabilities of VSAs: the binding operation and computing in superposition. In this paper, we introduce the algorithmic part of Hyperseed expressed within Fourier Holographic Reduced Representations VSA model, which is specifically suited for implementation on spiking neuromorphic hardware. The two distinctive novelties of the Hyperseed algorithm are: 1) Learning from only few input data samples and 2) A learning rule based on a single vector operation. These properties are demonstrated on synthetic datasets as well as on illustrative benchmark use-cases, IRIS classification and a language identification task using n -gram statistics.

Index Terms—self-organizing maps, vector symbolic architectures, hyperseed, neuromorphic hardware

I. INTRODUCTION

The use of Vector-Symbolic Architectures (VSA) in the machine learning and robotics context is currently gaining a great momentum [1]–[6]. In classification tasks, the use of VSA leads to order of magnitude increase in energy efficiency of computations on the one hand and natively enables one-shot and multitask learning on the other [7]. It is prospected that VSA will play a key role in the development of novel neuromorphic computer architectures [8] as an algorithmic abstraction [9], [10]. The main contribution of this paper is a novel algorithm for unsupervised learning called Hyperseed, which relies on the mathematical properties of arising from random representation spaces described through the concentration of measure [11] and of the main VSA operations of binding and bundling [12]. The method’s name suggests that data samples encoded as high-dimensional vectors (also called *hypervectors* or HVs), which are then mapped (aka “sowed”) onto a specially prepared topologically arranged set of hypervectors for revealing the internal cluster structure in the unlabeled data.

E. Osipov is with the Department of Computer Science, Electrical and Space Engineering at Luleå University of Technology, 97187 Luleå, Sweden. E-mail: Evgeny.Osipov@ltu.se

S. Kahawala, D. Haputhanthri, T. Kempitiya, D. De Silva and D. Alahakoon is with the Centre for Data Analytics and Cognition at La Trobe University, Melbourne, Australia. E-mail: {S.Kahawala, D.Haputhanthri, T.Kempitiya, D.DeSilva, D.Alahakoon} @latrobe.edu.au

D. Kleyko is with the Redwood Center for Theoretical Neuroscience at the University of California, Berkeley, CA 94720, USA and also with the Intelligent Systems Lab at Research Institutes of Sweden, 16440 Kista, Sweden. E-mail: denkle@berkeley.edu

The Hyperseed algorithm bears certain conceptual similarities to Kohonen’s Self-Organizing Map (SOM) algorithm [13], [14], however, it is designed using cardinally different computing principles. Therefore, certain SOM terminology is adopted for the description of our approach. Hyperseed implements the entire learning pipeline in terms of VSA operations. To the best of our knowledge, this has not been attempted prior and is reported for the first time.

The Hyperseed algorithm is presented using Frequency Holographic Reduced Representations (FHRR) [15] VSA model and the concept of fractional power encoding [15]–[17]. The usage of the FHRR model makes the proposed solution specifically fit for implementation on spiking neural network architectures including Intel’s Loihi [8].

To this end, we present the algorithmic part of Hyperseed and demonstrate its performance on three illustrative non-linear classification problems of varying complexity: Synthetic datasets from the Fundamental Clustering Problems Suite, Iris classification, and language identification using n -gram statistics. Across all experiments, Hyperseed convincingly demonstrates its key novelties of learning from a few input vectors and single vector operation learning rule, both of which contribute towards reduced time and computation complexity.

The paper is structured as follows. Section II describes the related work relevant to Hyperseed operations. The used methods including the fundamentals of VSA are presented in Section III. Section IV presents the main contribution – the method for unsupervised learning Hyperseed. Section V reports the results of the performance evaluation the experiments. Section VI discusses the suitability of Hyperseed for realization on neuromorphic hardware. The conclusions follow in Section VII .

II. RELATED WORK

VSA [12], [15], [18]–[20] is a computing framework providing methods of representing and manipulating concepts and their meanings in a high-dimensional space. VSA finds its applications in, for example, cognitive architectures [21], natural language processing [22]–[24], biomedical signal processing [1], [25], approximation of conventional data structures [26], [27], and for classification tasks such as gesture recognition [1], [28], cyber threat detection [29], physical activity recognition [30], fault isolation [31], [32]. Examples of efforts on using VSA for other than classification learning tasks are using data HVs for clustering [33]–[35], semi-supervised learning [36], collaborative privacy-

preserving learning [37], [38], multi-task learning [39], [40], distributed learning [41], [42].

Hypervectors of high (but fixed) dimensionality (denoted as d) are the basis for representing information in VSA. The information is distributed across hypervector positions, therefore, hypervectors use distributed representations [43]. There are different VSA models that all offer the same operation primitives but differ slightly in terms of the implementation of these primitives. For example, there are VSA models that compute with binary, bipolar [44], [45], continuous real, and continuous complex vectors [15]. Thus, the VSA concept has the flexibility to connect to a multitude of different hardware types, such as binary-valued VSAs for analog in-memory computing architectures [7] or complex-valued VSAs for spiking neuron architectures [46].

The relevant sub-domain of related work to the proposed Hyperseed algorithm is the application of VSA for solving machine learning tasks. In this context, VSA were used for: a) Representing input data and interfacing such representations with convolutional machine learning algorithms and b) Implementing the functionality of neural networks with VSA operations.

The most illustrative use cases for encoding of input data into hypervectors and interfacing convolutional machine learning algorithms are [34], [47]–[52]. For example, works [48], [50] proposed encoding n -gram statistics into hypervectors and subsequently solving typical natural language processing tasks with either supervised or unsupervised learning using standard artificial neural network architectures. The main distinctive property of VSA represented data is the substantial reduction of the memory footprint and the reduced of the learning time. In [34], hypervectors were used to encode sequences of variable lengths in the context of unsupervised learning of traffic patterns in intelligent transportation system application. In the context of visual navigation, hypervectors were used as input to Simultaneous Localization and Mapping (SLAM) algorithms [3].

A great potential of VSAs was demonstrated when used for the implementation of the entire functionality of classical neural network architectures. In [5], [53] the functionality of an entire class of randomly connected neural networks (random vector functional link networks and echo state networks) was implemented purely in terms of VSA operations. It was demonstrated that implementing the algorithm functionality with bipolar VSAs allows reducing energy consumption on the specialized digital hardware by the order of magnitude, while substantially decreasing the operation times.

III. METHOD: VECTOR SYMBOLIC ARCHITECTURES BASED ON HOLOGRAPHIC REDUCED REPRESENTATIONS

The Hyperseed algorithm is designed using the FHRR model [15]¹. The atomic FHRR hypervectors are randomly sampled from \mathbb{C}^d . Dimensionality d is a hyperparameter of Hyperseed.

¹The supplementary code base also contains the HRR implementation of the algorithm.

In high-dimensional random spaces, all random hypervectors are dissimilar to each other (quasi-orthogonal) with an extremely high probability. VSA defines operations and a similarity measure on hypervectors. In this paper, we use the cosine similarity for characterizing the similarity. Three key operations for computing with hypervectors are bundling, binding, and permutation.

A. Binding operation

The binding operation is used to bind two hypervectors together. The result of the binding is another hypervector. For example, for two hypervectors \mathbf{v}_1 and \mathbf{v}_2 the result of binding of their hypervectors (denoted as \mathbf{b}) is calculated as follows:

$$\mathbf{b} = \mathbf{v}_1 \circ \mathbf{v}_2, \quad (1)$$

where the notation \circ is used to denote the binding operation. In HRR, the binding operation is implemented as circular convolution of \mathbf{v}_1 and \mathbf{v}_2 , which can be implemented as the component-wise multiplication in the Fourier domain. This observation inspired FHRR where the representations are already in the Fourier domain in a form of phasors so that the component-wise multiplication, which is equivalent to the addition of phase angles modulo 2π , plays the role of the binding operation. There are two important properties of the binding operation. Firstly, the resultant hypervector \mathbf{b} is dissimilar to the hypervectors being bound, i.e., the similarity between \mathbf{b} and \mathbf{v}_1 or \mathbf{v}_2 is approximately 0. In FHRR, the similarity is measured as the mean of sum of cosines of angle differences.

Secondly, the binding operation preserves similarity. That is the distribution of the similarity measure between hypervectors from some set \mathcal{S} is preserved after binding of all hypervectors in \mathcal{S} with same random hypervector \mathbf{v} .

The binding operation is reversible. The unbinding, denoted as \oslash , is implemented by the circular correlation in HRR, which is in the case of FHRR is equivalent to component-wise multiplication with complex conjugate. Being the inverse of the binding operation, the unbinding obviously has the same similarity preservation property when performed on all hypervectors in \mathcal{S} with same hypervector \mathbf{v} .

$$\mathbf{v}_2 \oslash \mathbf{b} = \mathbf{v}_1 \quad (2)$$

B. Bundling operation

Bundling is denoted with $+$ and implemented via position-wise addition. The bundling operation combines several hypervectors into a single hypervector. For example, for hypervectors \mathbf{v}_1 and \mathbf{v}_2 the result of bundling (denoted as \mathbf{a}) is simply:

$$\mathbf{a} = \mathbf{v}_1 + \mathbf{v}_2. \quad (3)$$

In contrast to the binding operation, the resultant hypervector \mathbf{a} is similar to all bundled hypervectors, i.e., the cosine similarity between \mathbf{a} and \mathbf{v}_1 or \mathbf{v}_2 is larger than 0. Thus, the bundling operation allows storing information in hypervectors [54]. If

several copies of any hypervector are included (e.g., $\mathbf{a} = 3\mathbf{v}_1 + \mathbf{v}_2$), the resultant hypervector is more similar to the dominating hypervector than to other components.

If bundling is applied to several bindings it is possible to unbind any hypervector from any binding. In this case, the result of the operation is a noisy version of the second operand of the particular binding. For example, if $\mathbf{a} = \mathbf{v}_1 \circ \mathbf{v}_2 + \mathbf{u}_1 \circ \mathbf{u}_2$, then $\mathbf{u}_2 \circ \mathbf{a} = \mathbf{u}_1 + \text{noise} = \mathbf{u}_1^*$. Given that clean atomic hypervectors ($\mathbf{v}_1, \mathbf{v}_2, \mathbf{u}_1, \mathbf{u}_2$) are kept in an *item memory* and so vector \mathbf{u}_1^* is expected to have the highest similarity to \mathbf{u}_1 . Semantically, the same property holds for the binding of any atomic vector with the superposition of unbindings (which we use in the description of our approach). That is if $\mathbf{a} = \mathbf{v}_1 \circ \mathbf{v}_2 + \mathbf{u}_1 \circ \mathbf{u}_2$, then $\mathbf{u}_2 \circ \mathbf{a} = \mathbf{u}_1 + \text{noise} = \mathbf{u}_1^*$.

IV. HYPERSEED: UNSUPERVISED LEARNING WITH VECTOR SYMBOLIC ARCHITECTURES

This section presents the main contribution of this article – the method for unsupervised learning Hyperseed. Denote the set of FHRR-represented input data as $\mathcal{D} \in \mathbb{C}^d$. Denote as $\mathcal{P} \in \mathbb{C}^d$ the FHRR-represented points of a 2D grid, $|\mathcal{P}| = n \times m$, where n and m are the sizes of the grid along the vertical and the horizontal axes, respectively. For the sake of brevity, further in the text we will refer to set \mathcal{P} as HD-map.

The Hyperseed algorithm relies on the similarity preservation property of the (un)binding operation. It will project set \mathcal{D} onto set \mathcal{P} by unbinding all its members from hypervector \mathbf{s} , i.e.

$$\mathcal{D} \circ \mathbf{s} \Rightarrow \mathcal{P} \quad (4)$$

Hypervector \mathbf{s} is obtained as the result of the unsupervised learning rule. In essence, during the learning selected hypervectors from \mathcal{D} will be bound to selected vectors from \mathcal{P} as described further.

A. Initialization Phase: Generation of HD-map \mathcal{P} and hypervector \mathbf{s}

The hypervectors, which are the members of \mathcal{P} , are generated such that the similarity between them relates to topological proximity of points (also referred as nodes, in the sense of SOM, further on) on a 2D grid. Note, however, that the reference to the topological arrangement of \mathcal{P} is “virtual” and will be used for visualization purposes only.

The generation of the HD-map starts with two randomly generated unit hypervectors $\mathbf{x}_0, \mathbf{y}_0 \in \mathbb{C}^d$ as $\mathbf{x}_0 \sim e^{j \cdot 2\pi \cdot U(0,1)}$ and $\mathbf{y}_0 \sim e^{j \cdot 2\pi \cdot U(0,1)}$.

Let us denote the bandwidth parameter regulating the similarity between the adjacent coordinates on the grid by ϵ . The i 'th x and y coordinates of the grid will be created using the fractional power encoding [16], [55] as:

$$\mathbf{x}_i = \mathbf{x}_0^{\epsilon \cdot i}, \mathbf{y}_i = \mathbf{y}_0^{\epsilon \cdot i}. \quad (5)$$

The hypervector $\mathbf{p}_{(i,j)}$ representing a node with coordinates (i, j) on the grid is computed as $\mathbf{p}_{(i,j)} = \mathbf{x}_i \circ \mathbf{y}_j$. Fig. 1 shows similarity for the hypervector encoding coordinates (15, 15) on the 50×50 2D grid as a function of coordinates i and j .

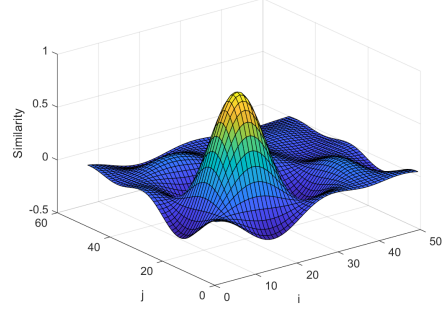


Fig. 1: Similarity distribution on an HD-map. The target node is (15, 15), the size of the grid is 50×50 , bandwidth $\epsilon = 0.05$.

Hypervector \mathbf{s} is initialized randomly as well: $\mathbf{s} \sim e^{j \cdot 2\pi \cdot U(0,1)}$. It is updated over several iterations during the learning phase as described in the next sections. The number of iterations is a hyperparameter of Hyperseed.

B. Search procedure in Hyperseed: Finding Best Matching Vector on the HD-map

In the Hyperseed algorithm, HD-map \mathcal{P} acts as an auto-associative memory [56]. That is the only operation performed on the HD-map is the search for the Best Matching Vector (BMV) given some input hypervector. The BMV is found by computing the cosine similarity between the input hypervector and all hypervectors in \mathcal{P} . The output of this procedure is a valid hypervector in \mathcal{P} with the highest similarity to the input hypervector.

The mapping ($\mathbf{d}_i \rightarrow \mathbf{p}_i$) of data hypervectors in \mathcal{D} to hypervectors of HD-map \mathcal{P} is done by unbinding \mathbf{d}_i from learned hypervector \mathbf{s} :

$$\mathbf{p}_i^* = \mathbf{d}_i \circ \mathbf{s}. \quad (6)$$

In (6) \mathbf{p}_i^* is a noisy version of a hypervector in \mathcal{P} .

C. Update phase: Unsupervised learning of hypervector \mathbf{s}

The goal with the update procedure on each iteration is to map input hypervector \mathbf{d}_i as near as possible to some target hypervector in \mathcal{P} with respect to cosine similarity metric.

Therefore, learning on a single iteration consists of three steps:

- 1) Choose a target hypervector \mathbf{p}_{target} (see the next subsection);
- 2) Compute a hypervector for perfect mapping $\mathbf{d}_i \rightarrow \mathbf{p}_{target}$ by binding of \mathbf{d}_i with \mathbf{p}_{target} .
- 3) Update hypervector \mathbf{s} by adding this perfect mapping hypervector to hypervector \mathbf{s} :

$$\mathbf{s} = \mathbf{s} + \mathbf{d}_i \circ \mathbf{p}_{target}. \quad (7)$$

Note that after the update \mathbf{s} is not a phasor vector anymore so it might be renormalized if necessary. Thus, by the end of the learning phase, hypervector \mathbf{s} is a bundle of bindings $\mathbf{d}_i \circ \mathbf{p}_j$.

As such, the result of future unbinding of hypervectors cosine-similar to \mathbf{d}_i used during the update with hypervector \mathbf{s} (6) is cosine-closer to hypervectors in \mathcal{P} used as target hypervectors during the update.

D. Looser-Takes-All phase: Finding a data hypervector for the update in a single iteration

The update rule (7) implies that the accuracy of retrieving \mathbf{p} 's by applying (6) for data hypervectors will decrease with the number of bindings inside \mathbf{s} hypervector. Therefore, \mathbf{s} should be updated only for few selected \mathbf{d}_i . In Hyperseed, data hypervector \mathbf{d}_i , which will be used for the update of \mathbf{s} is found during a special procedure.

Functionally, this procedure is the opposite of the Winner-Takes-All (WTA) procedure of Self-Organizing Maps. We, therefore, further refer to this procedure as Looser-Takes-All or LTA.

In the LTA procedure, the algorithm performs following steps:

- 1) Select a subset of data hypervectors from the training dataset² \mathcal{T} .
- 2) For each hypervector in \mathcal{T} compute the similarity to BMV using the search procedure described above.
- 3) Find the hypervector from \mathcal{T} , which unbinds \mathbf{p}^* with the lowest similarity to $\mathbf{p} \in \mathcal{P}$.

The hypervector from \mathcal{T} found at the end of the LTA procedure will be used for the update of hypervector \mathbf{s} in (7).

E. Finding the target node: Determining the target node on the HD-map

The hypervector found during the LTA procedure must be anchored to a hypervector \mathbf{p}_{target} , encoding a node on the HD-map. Since the LTA procedure finds a vector, which unbinds a node on the HD-map with the lowest similarity, intuitively, it should be bound to a different node. This new node should be located further away from the current BMV in order to create a new attractor for this and other cosine-similar input hypervectors.

To understand the rule for finding the new attractor node for the LTA-found input hypervector one needs to take into consideration the mathematical properties of the learning rule (7) and the hypervectors of sets \mathcal{D} and \mathcal{P} . We formulate the problem of finding such a rule by considering a simplified case where \mathbf{s} is constructed of two bindings for hypervectors $\mathbf{d}_1 = e^{j \cdot 2\pi \cdot \phi_1}$, $\mathbf{d}_2 = e^{j \cdot 2\pi \cdot \phi_2}$ with two nodes on the HD-map with coordinates (k, l) and $(k + \delta_x, l + \delta_y)$ on some offset δ_x and δ_y along x and y axes of the HD-map correspondingly. Then hypervector \mathbf{p}_1 encoding node (k, l) according to (5) is $\mathbf{p}_1 = e^{j \cdot 2\pi \cdot (r_k \cdot k + r_l \cdot l)}$ and hypervector \mathbf{p}_2 encoding node $(k + \delta_x, l + \delta_y)$ is $\mathbf{p}_2 = e^{j \cdot 2\pi \cdot (r_k \cdot (k + \delta_x) + r_l \cdot (l + \delta_y))}$, where $r_k = U(0, 1)$ and $r_l = U(0, 1)$ are random initial phase vectors of set \mathcal{P} . Hypervector \mathbf{s} after two updates is, therefore, $\mathbf{s} = e^{j \cdot 2\pi \cdot (r_k \cdot k + r_l \cdot l + \phi_1)} + e^{j \cdot 2\pi \cdot (r_k \cdot (k + \delta_x) + r_l \cdot (l + \delta_y) + \phi_2)}$. Assume now we unbind some vector $\mathbf{d}_3 = e^{j \cdot 2\pi \cdot \phi_3}$. This is done

by unbinding \mathbf{s} with complex conjugate of \mathbf{d}_3 , that is $\mathbf{d}_3 \odot \mathbf{s} = e^{j \cdot 2\pi \cdot (r_k \cdot k + r_l \cdot l + \phi_1 - \phi_3)} + e^{j \cdot 2\pi \cdot (r_k \cdot (k + \delta_x) + r_l \cdot (l + \delta_y) + \phi_2 - \phi_3)}$.

Now, depending on whether \mathbf{d}_3 is cosine-closer to either \mathbf{d}_1 or \mathbf{d}_2 the result of unbinding will be stronger attracted to either \mathbf{p}_1 or \mathbf{p}_2 . The other bindings in \mathbf{s} will introduce noise, which results in the displacement of the BMV on the HD-map. The exact position of the BMV \mathbf{p}_3 for \mathbf{d}_3 depends on several parameters: The bandwidth parameter ϵ , which determines the similarity layout of hypervectors in \mathcal{P} ; The choice of the offset for the placement of the target node δ_x and δ_y , which determines the strength of the influence from other bindings in \mathbf{s} ; and The phase of hypervectors \mathbf{d}_i from \mathcal{D} . Finding this attraction function analytically is non-trivial. We leave its theoretical investigation outside the scope for this article and instead focus on the practical considerations.

Practically, it is important to define a rule for selecting offsets δ_x and δ_y . Empirical results show that there exist different strategies for choosing \mathbf{p}_{target} . Primarily, the choice of the particular strategy affects the ‘‘visual’’ quality of projections on the HD-map.

The simplest from the implementation perspective rule is to randomly select the target hypervector \mathbf{p}_{target} . As we demonstrate in the next section this strategy leads to adequate accuracy performance of Hyperseed in classification tasks. At the same time, obviously, visualization of such projections is not very informative since it does not adequately display the internal structure of classes.

Another strategy is to choose target nodes on the HD-map according to a certain pattern. Fig. 2 and 3 demonstrate the instances of projections of the Iris dataset and a dataset containing collection of n -gram statistics from texts on seven European languages. Both datasets are projected onto a 20×20 HD-map. The complete experiment description follows in the next section.

In the figures, crosses show the choice of target nodes during the update procedure. Fig. 2 shows the projection of the Iris dataset after three updates with the target nodes placed on x -axis at coordinates $(0, 0)$, $(0, 10)$, $(0, 20)$. Fig 3 shows the projection of texts on seven European languages encoded by n -gram statistics of sentences after (only) four updates with the target nodes placed in the corners of the HD-map, that is $(0, 0)$, $(20, 0)$, $(20, 20)$ and $(0, 20)$. In both cases we see perfectly meaningful projections. The color of the crosses in both cases corresponds to the class of the hypervector selected by the LTA procedure.

Two most important observation one makes at this point are: 1.) The BMVs after the update procedures are different from the ones used in the update procedure and 2.) The classes that were not used for the update of vector \mathbf{s} , e.g., the class marked by green triangles from the Iris dataset and (Swedish, French, and Bulgarian) languages from the other dataset, emerge automatically and adequately projected reflecting the inner structure of data.

F. The iterative Hyperseed algorithm

In this section, we summarise the description of the Hyperseed algorithm by presenting its pseudo-code containing all

²In the case of online learning, there is an observation time parameter during which the observation phase operates.

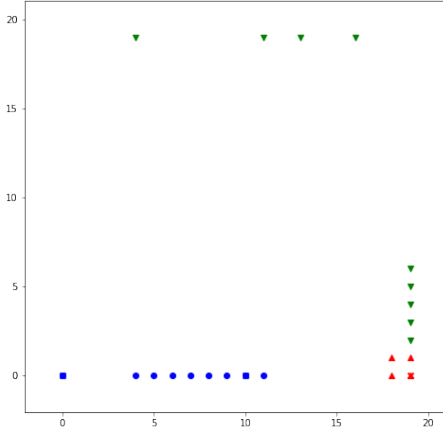


Fig. 2: Projection of Iris dataset after three updates. The chosen \mathbf{p}_{target} hypervectors are for nodes (0,0), (0,10), (0,20) marked by crosses.

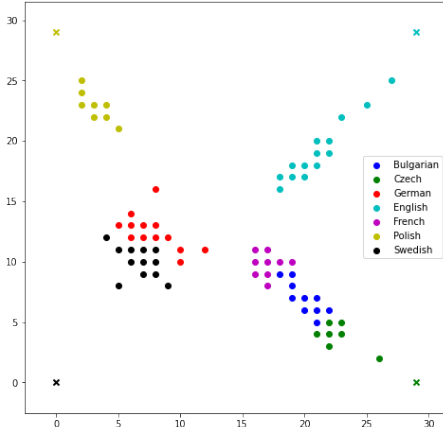


Fig. 3: Projection of seven European languages after four updates. The chosen \mathbf{p}_{target} hypervectors are for nodes (0,0), (20,0), (20,20) and (0,20).

phases. The important peculiarity of the learning procedure with Hyperseed is that only a random subset \mathcal{T}_i of the training data in \mathcal{D} of substantially smaller size is used in each iteration. The size of the training set is a hyperparameter of Hyperseed. During the experimental evaluation different strategies for setting the size of \mathcal{T}_i are demonstrated ranging from setting it to a constant to dynamically incrementing it with every iteration. Importantly, that independently of the chosen strategy, the size of set \mathcal{T}_i is substantially smaller than the size of the available training data ($|\mathcal{T}_i| \ll |\mathcal{D}|$). This is the unique property of the Hyperseed’s learning, it only takes few examples to the update phase.

The stop criterion to end the learning is the maximum number of iterations, which is a configurable parameter.

V. EXPERIMENTAL RESULTS

This section describes the results of the experimental evaluation of the proposed Hyperseed. We report three illustrative cases: 1) Unsupervised learning from one-shot demonstrations on six synthetic datasets; 2) Iris classification; and 3) 21

Algorithm 1 Iterative Hyperseed Learning

```

procedure HYPERSEEDLEARNING
   $i \leftarrow 1$  ▷ iteration counter
   $NumIter$  ▷ Max number of iterations
   $\mathcal{T}_i$  ▷ Subset of training hypervectors
  while  $i \leq NumIter$  do
     $Size\mathcal{T}_i$  ▷ A hyperparameter
     $\mathcal{T}_i \leftarrow SelectRandomlyFrom(\mathcal{D}, Size\mathcal{T}_i)$ 
     $\mathbf{d} \leftarrow LTA(\mathcal{T}_i)$  ▷ See Section IV-D
     $\mathbf{p} \leftarrow FIND\_TARGET(\mathcal{P})$  ▷ See Section IV-E
     $\mathbf{s} \leftarrow \mathbf{s} + \mathbf{d} \circ \mathbf{p}$  ▷ See Section IV-C

```

languages identification using n -gram statistics. In all the experiments, we used dense complex FHRR representations [57] with varying dimensionality. The Python implementation of the Hyperseed algorithm and the code necessary to reproduce all the experiments below are publicly available³.

A. Data transformation to high-dimensional space

In the first two experiments, where input data are in the form of feature vectors of size K , the values of each feature $f_k, k \in [1, K]$ were mean normalized. The range of values $[0, 1]$ was then quantized into q levels of equal size. For each feature a base unitary hypervector \mathbf{b}_k was randomly generated. Then levels for the particular feature \mathbf{I}_i^k were encoded in FHRR representation using fractional power encoding [16], [55], [58]: $\mathbf{I}_i^k = \mathbf{b}_k^{\epsilon_i}$, where $\epsilon \in \mathbb{R}$ represents the bandwidth parameter. The feature vector of a data sample was then represented as a single hypervector with the bundling operation: $\mathbf{v} = \sum_{k \in K} \mathbf{I}_i^k$.

In the language identification experiments, n -gram statistics was represented as hypervectors following the procedure in [50]. First, a bijection of the alphabet letters $i \in |\mathcal{A}|$ to random unitary atomic hypervectors \mathbf{b}_i was created. To encode the position of character i in the n -gram the permutation operation was used on the corresponding atomic hypervector \mathbf{b}_i . For example, the hypervector for character “b” on a third position in a tri-gram is the corresponding atomic hypervector rotated three times: $\rho^3(\mathbf{b}_b)$. An n -gram of size n was encoded as binding of position based encoded hypervectors for corresponding characters. For example, a tri-gram “bdf” was encoded as: $\rho(\mathbf{b}_b) \circ \rho^2(\mathbf{b}_d) \circ \rho^3(\mathbf{b}_f)$. The n -gram statistics for a given text sample is then encoded into a single hypervector by bundling hypervectors for all observed n -grams.

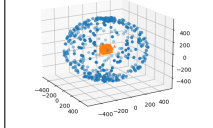
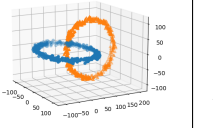
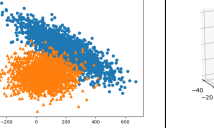
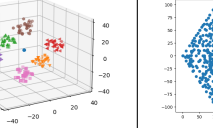
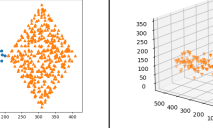
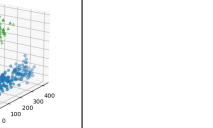
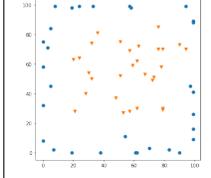
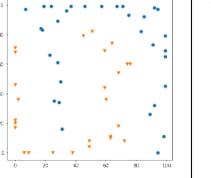
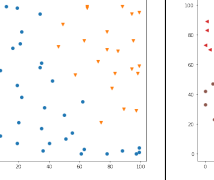
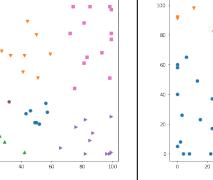
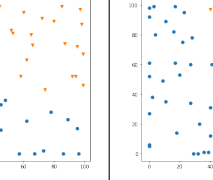
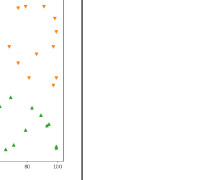
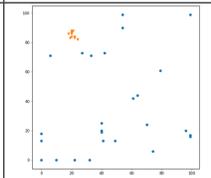
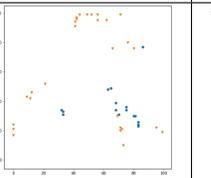
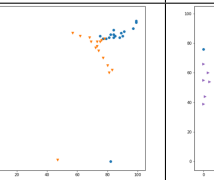
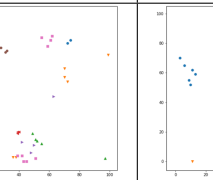
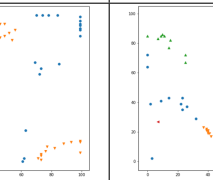
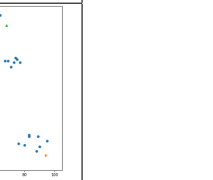
B. Hyperseed for Classification tasks

The proposed Hyperseed algorithm is by definition an unsupervised learning algorithm, therefore, an extra mechanism is needed to use it in supervised tasks such as the considered Iris classification and language identification task. Once Hyperseed was trained there is a need to assign labels to the best matching hypervectors in the HD-map.

Recall that Hyperseed is trained on a small subset of the available training data as described in Section IV-F. As will

³Implementation of Hyperseed and the experiments. [Online.] Available: <https://github.com/eaoltu/hyperseed>

TABLE I: Comparison of projections and classification accuracy of Hyperseed vs. Self-Organizing Maps on FCPS datasets

Dataset	Atom	Chain link	Engy time	Hepta	Two diamonds	Lsun 3D
						
SOM						
	Accuracy: 0.8878	Accuracy: 0.9265	Accuracy: 0.9528	Accuracy: 0.9777	Accuracy: 0.9774	Accuracy: 0.9715
Hyperseed						
	Accuracy: 0.9821	Accuracy: 0.9780	Accuracy: 0.9071	Accuracy: 0.9552	Accuracy: 0.9902	Accuracy: 0.9005

be demonstrated soon, each update of s hypervector creates not only a point of attraction for hypervectors similar to the one used for the updates, but also automatically reveals points of attractions for hypervectors, which are not part of the training subsets T_i . While for visual analytics related task small training subsets are sufficient, for classification tasks one need to expose the trained Hyperseed to more data in order to gather representative statistics of hit nodes on HD-map for all labels.

Therefore, for the labeling process in the presented below experiments the entire training dataset is presented to the trained Hyperseed HD-map for one full epoch that does not update the hypervector s . The labels of the training dataset are used to calculate statistics for the hit nodes in the HD-map. The nodes are assigned labels of the input samples that are prominent in the collected statistics.

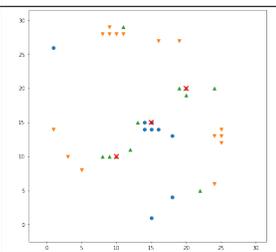
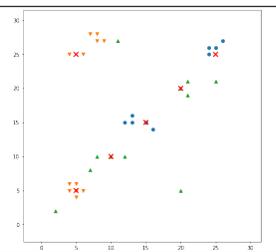
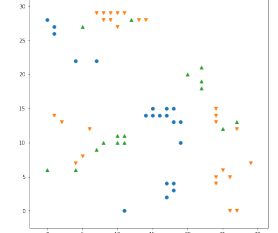
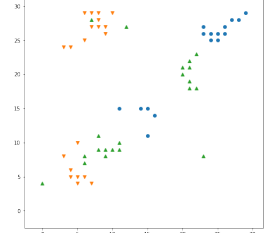
At the classification phase, hypervectors of the nodes with the assigned labels are stored in the memory. During the classification phase, samples of the test data are used to assess the trained Hyperseed. For each sample in the test data, the winning node on the HD-map is determined using the search procedure (Section IV-B). The test sample then is assigned the label of the closest labeled hypervector stored in the memory.

Accuracy is used as the main performance metric for evaluation and comparison of Hyperseed runs with different parameters. It should be emphasised that the focus of experiments is not on achieving the highest possible accuracy but on a comparative analysis of the Hyperseed algorithm.

C. Experiment 1: The performance of Hyperseed on synthetic datasets with one-shot demonstration

This experiment serves the purpose of highlighting the major property of the Hyperseed algorithm - the capability

TABLE II: Comparison of Hyperseed projections with different random seeds for IRIS dataset

	# updates: 3, Acc: 0.92	# updates: 6, Acc: 0.95
Train Projection		
Test Projection		

of one-shot learning. When talking about one-shot learning, one has to be careful with its definition. In many practical cases, a single example is obviously not enough for accurate inference, instead it is reasonable to talk about learning from a limited small number of examples, i.e., few-shot learning. This what we intend to gradually demonstrate with all three experiments.

In the first experiment, we fix the number of s hypervector updates to one. This essentially boils down to randomly picking a sample from the particular training set, running the Hyperseed's update phase and right after that performing labeling, classification on the corresponding test set, and the

visualization.

For this purpose, we use synthetic datasets from Fundamental Clustering Problems Suite (FCPS) [59]. FCPS provides several non-linear but simple datasets that can be visualized in two or three dimensions, for a variety of elementary benchmarking of clustering and non-linear classification algorithms.

We selected six FCPS datasets that are most representative of the non-linearity which we aim to learn using Hyperseed, they are: “Atom”, “ChainLink”, “EngyTime”, “Hepta”, “TwoDiamonds”, “Lsun3D”. We conducted the experiment eight times. In each run all hypervectors used for data encoding as well as for the operation of the Hyperseed algorithm was generated with a new seed.

In Table I, we present the results of this experiment as a comparative evaluation of the projections by the conventional SOM algorithm and the projections produced by the Hyperseed algorithm, both visually and as a classification accuracy metric for each dataset. The size of the SOM grid and the HD-map of the Hyperseed algorithm is the same 100×100 . The first row presents the visualization of the selected six datasets in their original two or three dimensional data space. The second row presents the HD-map projections and classification accuracy of the conventional SOM algorithm, while the third row shows the HD-map projections and classification accuracy of the Hyperseed algorithm.

The primary observation in relation to the classification is that the Hyperseed algorithm provided accuracy on a par with the conventional SOM (0.948 versus 0.943).

Secondly, the visualisation of the HD-map projections of Hyperseed are more representative of the topology preservation of the original data space, in comparison to the conventional SOM. In 3 out of 6 datasets, EngyTime, Hepta, and Lsun3D, the topology preservation is directly comparable to the original dataset, where inputs of the same category are tightly clustered in contrast to the conventional SOM where these inputs are more scattered. In the remaining three datasets, Atom, ChainLink and TwoDiamonds, although the topology preservation is not representative, the classification accuracy is high. This can be rationalised by the fixed 2D structure which inhibits the complete visualisation of the data space.

D. Experiment 2: Iris classification with Hyperseed

We proceed the demonstration by exploiting the details of Hyperseed’s functionality during several updates on the fixed size of the training set. We used Iris dataset with 150 samples of labeled data. The dataset contains three classes of Iris flowers described by four real-valued features. Data were encoded in hypervectors as described in Section V-A.

To further highlight the capabilities of Hyperseed to learn from few examples, we decided to split the Iris dataset such that the size of the testing part is larger than the size of the training part. The results for Hyperseed in this section were obtained for the 30%/70% split for training and testing, respectively. In order to give an immediate performance reference, we trained the conventional SOM algorithm with a 30 by 30 grid on different splits of the Iris dataset and counted the number of iterations it required for SOM to reach 95%

TABLE III: Number of iterations of the conventional SOM algorithm required to reach 95% accuracy for different splits of the Iris dataset.

Data set split (training/testing), in percent	30/70	40/60	60/40	80/20
Number of updates	-	2500	600	200

accuracy. The experiments with the conventional SOM were repeated 10 times and the maximum accuracy across runs was recorded. Table III demonstrates the results. One can see that for the 30/70 split the conventional SOM failed to achieve the target accuracy. Increasing the size of the test set allows SOM to reach the target accuracy. The number of required iterations, however, is large (the lowest is 200 for the 80/20 split). This time the maximum number of iterations of Hyperseed was set to 3 and 6. This means that algorithm performs 90 (3 times 30 samples of the training set) and 180 (6 times 30 samples of the training set) lookups for the Best Matching Vector and only 3 (and correspondingly 6) updates of s hypervector. This has to be compared to 200 times 120 of lookups and updates of the conventional SOM in the 80/20 split case. Each experiment (with three and six updates) was ran 10 times with random seeds. In each run all hypervectors used for data encoding as well as for the operation of the Hyperseed algorithm was generated with new seed.

The target nodes at each update were pre-selected to be (15,15) - for the first update, (20,20) - for the second update, (10,10) - for the third update, (5,5) - for the fourth update, (25,25) - for the fifth update and (5,25) - for the sixth update. These nodes are marked by red crosses when needed. It is important to observe that the visual projections with this placement of \mathbf{p}_{target} hypervectors are different from that in Figure 2. This highlights again the importance target node selection rule for visually adequate projections. In this experiment, however, the adequate visualization is not important since our focus is on the performance characteristics of the Hyperseed algorithm in the classification task. Table II shows the results of the experiment. For fair comparison with SOM here we also select the best performance across runs.

The first interesting observation comes in the three updates case. We selected best runs, which resulted in the highest accuracy on the test set (0.93). The projection of the train set show that out of three updates in total one update was done for class 1 (blue circles) and two updates were done for class two training samples. Similarly to what was observed previously in Figure 2 the cluster for class three emerged automatically.

Another important observation comes from the relative placement of the samples (both from the train and the test datasets) on HD-map. For Iris dataset it is known that classes two and three are very similar to each other, which manifests in miss classification of some of their samples. Here we see that this is indeed the case (orange triangles are very close to green triangles in several places of the map). However, in the case of Hyperseed this proximity does not lead to large degradation of the classification accuracy. This is because of each point in the HD-map becomes a strong attractor for similar samples.

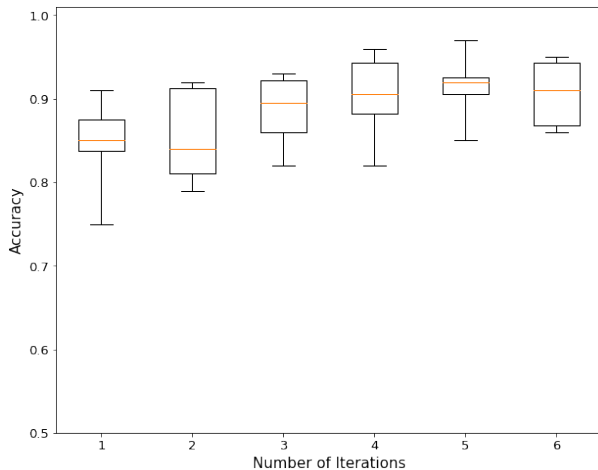


Fig. 4: Number of iterations vs accuracy ($d = 500$).

Next, Figure 4 shows the accuracy of Hyperseed with increasing number of updates. With increasing the number of updates the classification accuracy of Hyperseed on average improves.

E. Experiment 3: Training Hyperseed on n -grams in language identification task

While the previous two experiments were used to get first insights on the major properties of Hyperseed, with this experiment we intend to demonstrate its performance on a larger scale problem: we will use it for the classification task of 21 European languages using n -gram statistics. The list of languages is as follows: Bulgarian, Czech, Danish, German, Greek, English, Estonian, Finnish, French, Hungarian, Italian, Latvian, Lithuanian, Dutch, Polish, Portuguese, Romanian, Slovak, Slovene, Spanish, Swedish. The training data is based on the Wortschatz Corpora [60]. The average size of a language’s corpus in the training data were $1,085,637.3 \pm 121,904.1$ symbols. In this study we use the method for encoding n -gram statistics into hypervectors from [50], where it was used as an input to the conventional SOM algorithm. Each original language corpus was divided into samples where the length of each sample was set to 1,000 symbols. The total number of samples in the training data was 22,791.

The test data also contains samples from the same languages and is based on the Europarl Parallel Corpus⁴. The total number of samples in the test data was 21,000, where each language was represented with 1,000 samples. Each sample in the test data corresponds to a single sentence. The average size of a sample in the test data was 150.3 ± 89.5 symbols.

The data for each language was pre-processed such that the text included only lower case letters and spaces. All punctuation was removed. Lastly, all text used the 26-letter ISO basic Latin alphabet, i.e., the alphabet for both training and test data was the same and it included 27 symbols. For each text sample the n -gram statistics transformed to

hypervectors was obtained, which was then used as input when training or testing Hyperseed. Since each sample was preprocessed to use the alphabet of only $a = 27$ symbols, the conventional n -gram statistics input is 27^n dimensional. In the experiment we used tri-grams, therefore the conventional representation is 19,683 dimensional. The dimensionality of the mapped n -gram statistics into hypervectors as described in section V-A depends on the dimensionality of the hypervectors d . The reported below results were obtained for different dimensionalities in the range 400-10000, which corresponds to the dimensionality reduction of the original representation space from 49 folds (for $d = 400$) to 2 folds (for $d = 10,000$).

In this experiment, we used 100×100 HD-map. We also used an adaptive strategy for choosing the size of the training set used on each iteration. During the training process on each iteration we randomly sampled the original training set to construct an *observation* set of size $T_i = 3i$, where i is the iteration count. In this way, the size of the observation set increases with every iteration. For example after 10 iterations Hyperseed will be exposed to 156 randomly selected (with replacement) samples from the original 22,791 training samples. Note, however, that the labeling process was performed on the entire training set. This is done in order to enable emergence of new clusters from the previously unseen samples.

The first experiment was performed with dimensionality of hypervectors $d = 5,000$ (4 folds dimensionality reduction). In this experiment, we exposed Hyperseed to different number of classes from the original datasets. The number of Hyperseed updates in each case was set relative to the number of classes at hand. Importantly, this heuristic for choosing the number of updates is adopted for automating experiments only. It only reflects the desire of keeping the number of iterations low. In the supervised learning context the information about the number of classes is obviously unavailable.

The experiment was performed 8 times for each number of classes, each time selecting a different subset of languages for Hyperseed training. Fig. 5a show the result. The reference accuracy 0.97 (the red line) is the accuracy obtained with the conventional tri-gram representation reported in [61], [62] for using the nearest neighbor classifier.

The main observation to make here is that the performance of Hyperseed drops as it is being exposed to large number of classes. The explanation to this is connected to the finite capacity of hypervectors in terms of the number of hypervectors one can bundle together while keeping a sufficient accuracy of retrieving them back. As we discussed above, each update to hypervector s introduces noise to the previous updates. That is why the number of updates in Hyperseed needs to be kept low.

1) *Updated Hyperseed learning phase:* To mitigate the problem of the reduced accuracy in large scale (in terms of number of distinct classes) the learning phase of Hyperseed was updated.

Instead of having a single s hypervector it is proposed to use N vectors $s_i, i = 1..N$. N is another hyperparameter of Hyperseed. During the update procedures these hypervectors will be updated in a round-robin manner in order to keep the number of updates per hypervector balanced.

⁴Available online at <http://www.statmt.org/europarl/>.

During the search of the best matching vector in either LTA or the test procedures the binding in (1) is now computed for the current input hypervector and all hypervectors s_i 's.

Hypervector \mathbf{p} with the highest cosine similarity across all results of unbinding with all s_i is selected as BMV.

The number of iterations (and as the result the number of updates) with the new update phase should be scaled such that the number of updates per s_i hypervector is approximately same. For example in the experiments with $N = 10$ the number of iterations was configured to 30 to allow for 3 updates per s_i hypervector.

Fig. 5b shows significant performance improvement with the updated learning phase. The maximum performance of Hyperseed in 21 classes case is 0.91 after 30 iterations.

Next, we are interested in the effect of the number of s hypervectors hyperparameter on the performance of Hyperseed. Fig. 5c shows the classification accuracy in the 21 classes case for different number of s hypervectors used in the learning phase. The main observation here is that the performance stabilizes after certain value for this parameter. In our case there is no significant increase in the accuracy after using 10 s hypervectors.

2) *Hyperseed performance for different dimensionalities of hypervectors:* Finally, we are interested in the effect of the dimensionality of hypervectors on the performance of hyperseed. We performed an experiment with the number of s hypervectors fixed to 10 and vary the dimensionality of the hypervectors used by the algorithm from 400 until 10000. The results are shown in Fig. 5d. The main observation to make is that the classification accuracy on low dimensionalities is expectedly low. On the positive side it is substantially higher than the random choice, which is 0.04 in this case. The reason for this is rather clear and it is connected to the true dimensionality of the non-distributed representations, which is high (19, 683). With 400 dimensions and the adopted encoding procedure of the input we operate well above the capacity of the hypervectors, this leads to higher inter-class similarity. Increasing the dimensionality expectedly leads to better accuracy. It turns out that in the case of language classification 5,000 is the optimal dimensionality for obtaining acceptable results. It is worth noting that the accuracy of Hyperseed is 0.07 lower than the reference case, it is not expected that it necessarily achieve the highest accuracy compared to the supervised methods. The important advantage of the Hyperseed algorithm (similarly to SOM) is data visualization.

VI. DISCUSSION

There are several aspects of Hyperseed, which worth a discussion and require further investigation. In this section, we list the most important ones.

A. Hyperseed on neuromorphic hardware

The Hyperseed algorithm from the start was designed targeting an implementation on the neuromorphic hardware. This target departs from two recent works [46], [63], which demonstrated the feasibility of implementing an auto-associative memory and a similarity based nearest neighbor search using

distributed representations on Intel Loihi neuromorphic chip [8]. Connected to Hyperseed, an alert reader can realize that since the update procedure takes only few vector operations, the computational bottleneck of the algorithm is the search phase, where the Best Matching Vector on the HD-map is looked up for an unbound noisy vector \mathbf{p}^* in (6).

While the major focus of this paper is the algorithmic core of Hyperseed, here we want to give an indication of its performance when implemented on the neuromorphic hardware, which is a part of the ongoing development.

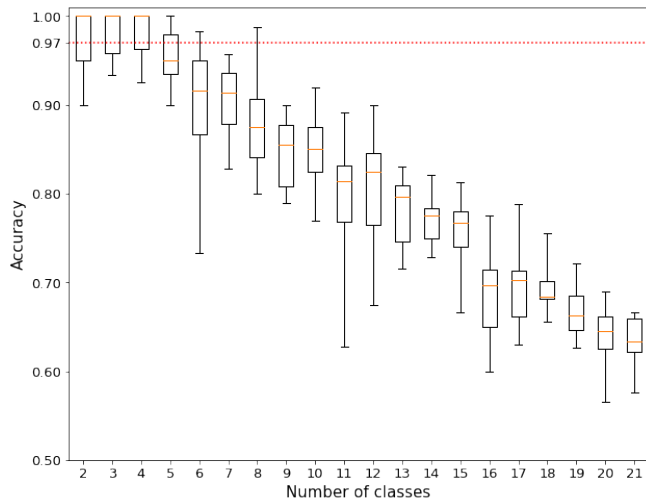
We used the existing implementation of k NN for Loihi from [63] to measure the performance of the Hyperseed's search phase in the language classification task. To do this, HD-maps of various sizes (starting from 30×30 and incrementing the grid size by 10 along each axis until size 90×90) were generated as described in Section IV-A. The vectors of each HD-map were then used for learning the spiking representation of the k NN reference base of the corresponding size on Intel's Loihi based Nahuku-32 neuromorphic system. It is important to note that this operation is performed only once at the initialization step. When learned the HD-map remains unchanged for the life time of Hyperseed. Therefore, the build time of the reference base was not taken into account in the run-time performance evaluation.

For the experiment we chose the case of classifying five randomly selected languages with a single *seed* vector as a reference case. The original dimensionality of the hypervectors used for the encoding of the input data as well as for all hypervectors of the Hyperseed algorithm was $d = 10000$. The reference case accuracy of Hyperseed obtained on a PC was 0.84.

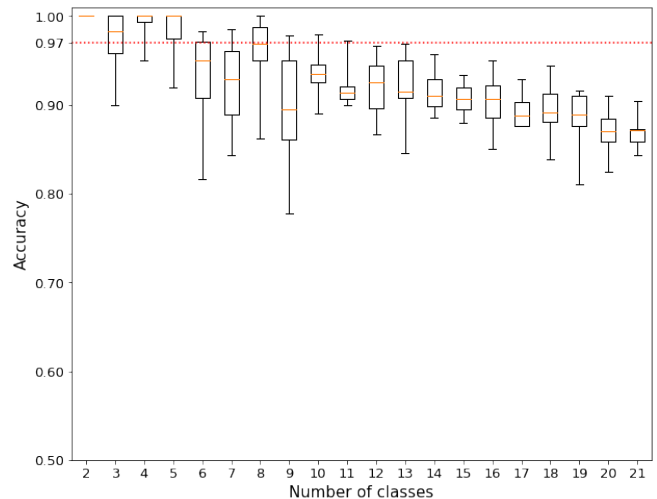
k NN on Loihi was used to model the search operation during the labeling and testing process. To do this *seed* vector was pre-trained offline on the PC as described in Section IV-C. For the labeling process binding of all training and test data with the trained *seed* hypervector was performed and the results (the noisy versions of the best matching vectors) were used as queries to the k NN reference base storing the hypervectors of the HD-map on Loihi. The dimensionality of the existing Loihi implementation of k NN is $d_{kNN} < 512$, which is a platform specific limit. In our experiments, in order to interface all hypervectors from the reference case to Loihi we reduced their dimensionality to $d = 400$ from the original using the PCA/ICA method.

To do the labeling of best matching vectors, the training data (after binding with *seed* vector) was used as queries to k NN and the top 1 index for each query (the earliest fired output neuron) was recorded. After that the labeling was performed on the PC using the procedure described above. To compute the accuracy, the test data hypervectors (also after binding with *seed* vector) were used as queries to k NN. The top 1 index was recorded and used to compute the accuracy against the list of the labeled indices obtained previously.

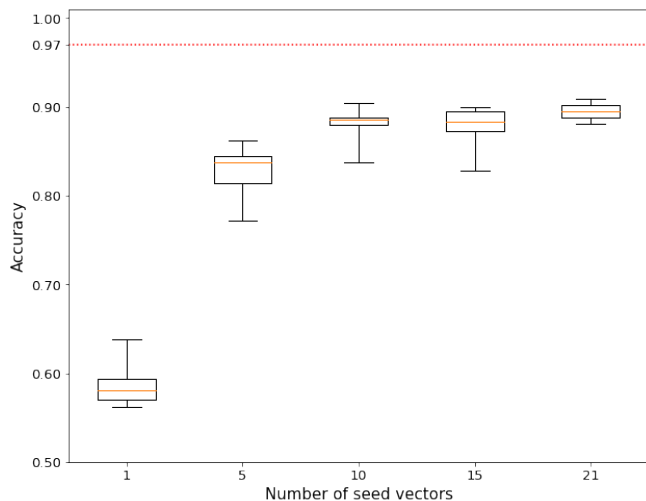
The average measured accuracy on Loihi was 0.84, which is the same as the reference accuracy measured on the PC implementation of Hyperseed. This means that the spiking implementation of the HD-map and the dot product calculation does not introduce sensible errors.



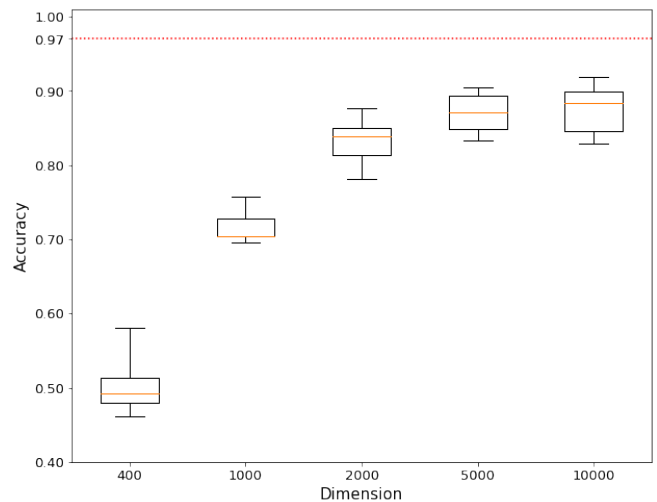
(a) Accuracy with single s hypervector (original update rule from Section IV-C) ($d = 5000$).



(b) Number of classes vs. accuracy with original and modified learning phases ($d = 5000$).



(c) Number of s hypervectors vs. accuracy ($d = 5000$).



(d) Dimensionality of hypervectors vs. accuracy (Number of s hypervectors is 10).

Fig. 5: Results of Experiment 3. Performance of Hyperseed in 21 languages classification task.

Next, in addition to the accuracy we also measured the query time to k NN reference base for different sizes of HD-map. The main outcome of this experiment is illustrated in Fig. 6. It shows the computational benefit of implementing the bottleneck operation of Hyperseed on a neuromorphic computing platform: Due to parallel, power-efficient computation of the dot product in Loihi, Hyperseed as expected is empowered with constant-time search for different sizes of the HD-map.

B. The importance of good embeddings into hyperdimensional representations

While a large body of knowledge on methods for encoding objects into hypervectors is accumulated throughout the years, the problem is still considered as of the primary importance in the area of hyperdimensional computing. Hyperseed in this respect offers a playground for comparing different embeddings as the good quality embeddings lead to higher accuracy

in the classification task. Connected to the previous topic, it is particularly important to develop the operations of Hyperseed on sparse representations.

C. Hyperseed in the multitask learning context

The usage of VSA in the multi-task learning context has recently gained an increased attention. The recent works [2], [4], [39], [40], [64] proposed using context hypervectors for multi-task hypervectors in the supervised learning concept. The usage of context hypervectors with Hyperseed is natural. By applying context binding to the best matching vectors of the HD-map one obtains unique context-specific symbolic representations which could be used as an input to long-term memory architectures such as Sparse Distributed Memory [65]. In our opinion, this direction is worth investigating in the context of cognitive architectures.

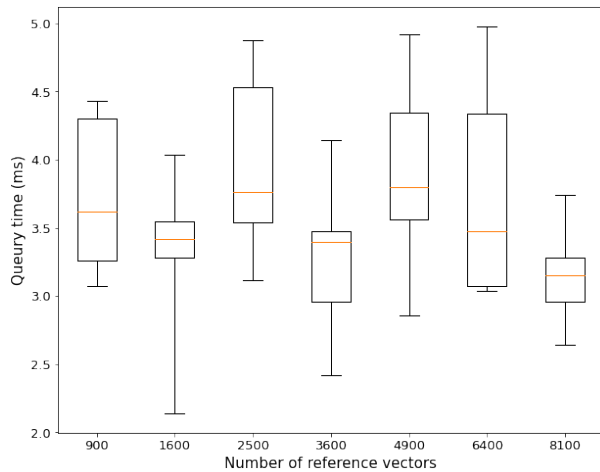


Fig. 6: Time of querying a noisy best matching vector in an HD-map implemented as a k NN reference base vs. size of the HD-map in number of reference vectors.

VII. CONCLUSIONS

The increasing accumulations of unstructured and unlabelled big data has initiated a renewed interest in unsupervised machine learning algorithms that are able to capitalize on computational efficiencies of biologically inspired neuromorphic hardware. In this paper, we have presented the Hyperseed algorithm that addresses these challenges through the manifestation of a novel unsupervised learning approach that leverages VSA for fast learning from only few input vectors and single vector operation learning rule implementation. A further novelty is that it implements the entire learning pipeline purely in terms of VSA operations. Hyperseed has been empirically evaluated across diverse scenarios: synthetic datasets from Fundamental Clustering Problems Suite, benchmark classification using the Iris dataset, and the more practical classification of 21 European languages using n -gram statistics. Results of all experiments confirm the learning performance, quality of learning outcomes, and robustness of the Hyperseed algorithm. As future work, we intend to implement all operations of Hyperseed on neuromorphic hardware, followed by its application for unsupervised learning of Internet of Things data streams on low-energy Edge computing devices.

VIII. ACKNOWLEDGEMENTS

This work was supported by the Intel Neuromorphic Research Community Grant to Luleå University of Technology. The work of DK was supported by the European Union's Horizon 2020 Programme under the Marie Skłodowska-Curie Individual Fellowship Grant (839179).

REFERENCES

- [1] A. Rahimi, P. Kanerva, L. Benini, and J. M. Rabaey, "Efficient Biosignal Processing Using Hyperdimensional Computing: Network Templates for Combined Learning and Classification of ExG Signals," *Proceedings of the IEEE*, vol. 107, no. 1, pp. 123–143, 2019.
- [2] B. Cheung, A. Terekhov, Y. Chen, P. Agrawal, and B. Olshausen, "Superposition of Many Models into One," in *Advances in Neural Information Processing Systems (NIPS)*, 2019, pp. 10 868–10 877.

- [3] P. Neubert, S. Schubert, and P. Protzel, "An Introduction to Hyperdimensional Computing for Robotics," *KI - Künstliche Intelligenz*, vol. 33, no. 4, pp. 319–330, 2019.
- [4] M. Hersche, P. Rupp, L. Benini, and A. Rahimi, "Compressing Subject-specific Brain-Computer Interface Models into One Model by Superposition in Hyperdimensional Space," in *Design, Automation Test in Europe Conference Exhibition (DATE)*, 2020, pp. 246–251.
- [5] D. Kleyko, M. Kheffache, E. P. Frady, U. Wiklund, and E. Osipov, "Density encoding enables resource-efficient randomly connected neural networks," *IEEE Transactions on Neural Networks and Learning Systems*, vol. 32, no. 8, pp. 3777–3783, 2021.
- [6] P. Neubert and S. Schubert, "Hyperdimensional Computing as a Framework for Systematic Aggregation of Image Descriptors," in *Conference on Computer Vision and Pattern Recognition (CVPR)*, 2021, pp. 16 938–16 947.
- [7] G. Karunaratne, M. L. Gallo, G. Cherubini, L. Benini, A. Rahimi, and A. Sebastian, "In-Memory Hyperdimensional Computing," *Nature Electronics*, vol. 3, no. 6, pp. 327–337, 2020.
- [8] M. Davies, N. Srinivasa, T.-H. Lin, G. Chinya, Y. Cao, S. H. Choday, G. Dimou, P. Joshi, N. Imam, S. Jain, Y. Liao, C.-K. Lin, A. Lines, R. Liu, D. Mathaikutty, S. McCoy, A. Paul, J. Tse, G. Venkataramanan, Y.-H. Weng, A. Wild, Y. Yang, and H. Wang, "Loihi: A Neuromorphic Manycore Processor with On-Chip Learning," *IEEE Micro*, vol. 38, no. 1, pp. 82–99, 2018.
- [9] A. Rahimi, S. Datta, D. Kleyko, E. P. Frady, B. Olshausen, P. Kanerva, and J. M. Rabaey, "High-dimensional Computing as a Nanoscale Paradigm," *IEEE Transactions on Circuits and Systems I: Regular Papers*, vol. 64, no. 9, pp. 2508–2521, 2017.
- [10] D. Kleyko, M. Davies, E. P. Frady, P. Kanerva, S. J. Kent, B. A. Olshausen, E. Osipov, J. M. Rabaey, D. A. Rachkovskij, A. Rahimi, and F. T. Sommer, "Vector Symbolic Architectures as a Computing Framework for Nanoscale Hardware," *arXiv:2106.05268*, pp. 1–28, 2021.
- [11] A. N. Gorban and I. Y. Tyukin, "Blessing of Dimensionality: Mathematical Foundations of the Statistical Physics of Data," *Philosophical Transactions of the Royal Society A: Mathematical, Physical and Engineering Sciences*, vol. 376, no. 2118, pp. 1–18, 2018.
- [12] P. Kanerva, "Hyperdimensional computing: An introduction to computing in distributed representation with high-dimensional random vectors," *Cognitive Computation*, vol. 1, no. 2, pp. 139–159, 2009.
- [13] T. Kohonen, *Self-Organizing Maps*. Springer Series in Information Sciences, 2001.
- [14] D. Kleyko, E. Osipov, D. D. Silva, U. Wiklund, and D. Alahakoon, "Integer self-organizing maps for digital hardware," in *2019 International Joint Conference on Neural Networks (IJCNN)*, 2019, pp. 1–8.
- [15] T. A. Plate, *Holographic Reduced Representations: Distributed Representation for Cognitive Structures*. Stanford: Center for the Study of Language and Information (CSLI), 2003.
- [16] E. P. Frady, D. Kleyko, C. J. Kymn, B. A. Olshausen, and F. T. Sommer, "Computing on Functions Using Randomized Vector Representations," *arXiv:2109.03429*, pp. 1–33, 2021.
- [17] B. Komer, T. C. Stewart, A. R. Voelker, and C. Eliasmith, "A Neural Representation of Continuous Space using Fractional Binding," in *Annual Meeting of the Cognitive Science Society (CogSci)*, 2019, pp. 2038–2043.
- [18] D. A. Rachkovskij, "Representation and Processing of Structures with Binary Sparse Distributed Codes," *IEEE Transactions on Knowledge and Data Engineering*, vol. 3, no. 2, pp. 261–276, 2001.
- [19] A. Rahimi, S. Datta, D. Kleyko, E. P. Frady, B. Olshausen, P. Kanerva, and J. M. Rabaey, "High-dimensional Computing as a Nanoscale Paradigm," *IEEE Transactions on Circuits and Systems I: Regular Papers*, vol. , no. , pp. 1–14, 2017.
- [20] E. P. Frady, D. Kleyko, and F. T. Sommer, "Variable Binding for Sparse Distributed Representations: Theory and Applications," *IEEE Transactions on Neural Networks and Learning Systems*, vol. PP, no. 99, pp. 1–14, 2021.
- [21] C. Eliasmith, *How to Build a Brain*. Oxford University Press, 2013.
- [22] M. N. Jones and D. J. K. Mewhort, "Representing Word Meaning and Order Information in a Composite Holographic Lexicon," *Psychological Review*, vol. 114, no. 1, pp. 1–37, 2007.
- [23] G. Recchia, M. Sahlgren, and P. K. M. Jones, "Encoding Sequential Information in Semantic Space Models. Comparing Holographic Reduced Representation and Random Permutation," *Computational Intelligence and Neuroscience*, pp. 1–18, 2015.
- [24] D. Kleyko, E. Osipov, and R. Gayler, "Recognizing Permuted Words with Vector Symbolic Architectures: A Cambridge Test for Machines," *Procedia Computer Science*, vol. 88, pp. 169–175, 2016.

- [25] D. Kleyko, E. Osipov, and U. Wiklund, "A Hyperdimensional Computing Framework for Analysis of Cardiorespiratory Synchronization During Paced Deep Breathing," *IEEE Access*, vol. 7, pp. 34 403–34 415, 2019.
- [26] E. Osipov, D. Kleyko, and A. Legalov, "Associative Synthesis of Finite State Automata Model of a Controlled Object with Hyperdimensional Computing," in *Annual Conference of the IEEE Industrial Electronics Society (IECON)*, 2017, pp. 3276–3281.
- [27] D. Kleyko, A. Rahimi, R. Gayler, and E. Osipov, "Autoscaling Bloom Filter: Controlling Trade-off Between True and False Positives," *Neural Computing and Applications*, pp. 1–10, 2019.
- [28] D. Kleyko, A. Rahimi, D. Rachkovskij, E. Osipov, and J. Rabaey, "Classification and Recall with Binary Hyperdimensional Computing: Trade-offs in Choice of Density and Mapping Characteristic," *IEEE Transactions on Neural Networks and Learning Systems*, vol. PP, no. 99, pp. 1–19, 2018.
- [29] V. Christopher, T. Aathman, K. Mahendrakumaran, R. Nawaratne, D. De Silva, V. Nanayakkara, and D. Alahakoon, "Minority resampling boosted unsupervised learning with hyperdimensional computing for threat detection at the edge of internet of things," *IEEE Access*, 2021.
- [30] O. Rasanen and S. Kakouros, "Modeling dependencies in multiple parallel data streams with hyperdimensional computing," *IEEE Signal Processing Letters*, vol. 21, no. 7, pp. 899–903, 2014.
- [31] D. Kleyko, E. Osipov, N. Papakonstantinou, and V. Vyatkin, "Hyperdimensional Computing in Industrial Systems: The Use-Case of Distributed Fault Isolation in a Power Plant," *IEEE Access*, vol. 6, pp. 30 766–30 777, 2018.
- [32] M. Eggimann, A. Rahimi, and L. Benini, "A 5 μ W Standard Cell Memory-based Configurable Hyperdimensional Computing Accelerator for Always-on Smart Sensing," *arXiv:2102.02758*, pp. 1–14, 2021.
- [33] M. Imani, Y. Kim, T. Worley, S. Gupta, , and T. Rosing, "HDCluster: An Accurate Clustering Using Brain-Inspired High-Dimensional Computing," in *Design, Automation Test in Europe Conference Exhibition (DATE)*, 2019, pp. 1591–1594.
- [34] T. Bandaragoda, D. D. Silva, D. Kleyko, E. Osipov, U. Wiklund, and D. Alahakoon, "Trajectory Clustering of Road Traffic in Urban Environments using Incremental Machine Learning in Combination with Hyperdimensional Computing," in *IEEE Intelligent Transportation Systems Conference (ITSC)*, 2019, pp. 1664–1670.
- [35] A. Hernández-Cano, Y. Kim, and M. Imani, "A Framework for Efficient and Binary Clustering in High-Dimensional Space," in *Design, Automation Test in Europe Conference Exhibition (DATE)*, 2021, pp. 1859–1864.
- [36] M. Imani, S. Bosch, M. Javaheripi, B. D. Rouhani, X. Wu, F. Koushanfar, and T. Rosing, "SemiHD: Semi-Supervised Learning Using Hyperdimensional Computing," in *IEEE/ACM International Conference on Computer-Aided Design (ICCAD)*, 2019, pp. 1–8.
- [37] M. Imani, Y. Kim, S. Riazi, J. Messerly, P. Liu, F. Koushanfar, and T. Rosing, "A Framework for Collaborative Learning in Secure High-Dimensional Space," in *IEEE International Conference on Cloud Computing (CLOUD)*, 2019, pp. 435–446.
- [38] B. Khaleghi, M. Imani, and T. Rosing, "Prive-HD: Privacy-Preserved Hyperdimensional Computing," in *ACM/ESDA/IEEE Design Automation Conference (DAC)*, 2020, pp. 1–6.
- [39] C.-Y. Chang, Y.-C. Chuang, and A.-Y. A. Wu, "Task-Projected Hyperdimensional Computing for Multi-task Learning," in *IFIP International Conference on Artificial Intelligence Applications and Innovations (AIAI)*, ser. IFIP Advances in Information and Communication Technology, vol. 583, 2020, pp. 241–251.
- [40] —, "IP-HDC: Information-Preserved Hyperdimensional Computing for Multi-Task Learning," in *IEEE Workshop on Signal Processing Systems (SiPS)*, 2020, pp. 1–6.
- [41] A. Rosato, M. Panella, and D. Kleyko, "Hyperdimensional Computing for Efficient Distributed Classification with Randomized Neural Networks," in *International Joint Conference on Neural Networks (IJCNN)*, 2021, pp. 1–10.
- [42] C.-Y. Hsieh, Y.-C. Chuang, and A.-Y. A. Wu, "FL-HDC: Hyperdimensional Computing Design for the Application of Federated Learning," in *IEEE International Conference on Artificial Intelligence Circuits and Systems (AICAS)*, 2021, pp. 1–5.
- [43] G. Hinton, J. McClelland, and D. Rumelhart, "Distributed Representations," in *Parallel Distributed Processing. Explorations in the Microstructure of Cognition. Volume 1. Foundations*, D. Rumelhart and J. McClelland, Eds. MIT Press, 1986, pp. 77–109.
- [45] R. W. Gayler, "Multiplicative binding, representation operators & analogy," in *Gentner, D., Holyoak, K. J., Kokinov, B. N. (Eds.), Advances in analogy research: Integration of theory and data from the cognitive, computational, and neural sciences*, New Bulgarian University, Sofia, Bulgaria, 1998, pp. 1–4.
- [46] E. P. Frady and F. T. Sommer, "Robust Computation with Rhythmic Spike Patterns," *Proceedings of the National Academy of Sciences*, vol. 116, no. 36, pp. 18 050–18 059, 2019.
- [47] D. A. Rachkovskij, "Linear Classifiers based on Binary Distributed Representations," *Information Theories and Applications*, vol. 14, no. 3, pp. 270–274, 2007.
- [48] P. Alonso, K. Shridhar, D. Kleyko, E. Osipov, and M. Liwicki, "HyperEmbed: Tradeoffs Between Resources and Performance in NLP Tasks with Hyperdimensional Computing enabled Embedding of n-gram Statistics," in *International Joint Conference on Neural Networks (IJCNN)*, 2021, pp. 1–9.
- [49] F. Mirus, P. Blouw, T. C. Stewart, and J. Conradt, "An investigation of vehicle behavior prediction using a vector power representation to encode spatial positions of multiple objects and neural networks," *Frontiers in Neuroinformatics*, vol. 13, pp. 1–17, 2019.
- [50] D. Kleyko, E. Osipov, D. D. Silva, U. Wiklund, V. Vyatkin, and D. Alahakoon, "Distributed Representation of n-gram Statistics for Boosting Self-Organizing Maps with Hyperdimensional Computing," in *International Andrei Ershov Memorial Conference on Perspectives of System Informatics (PSI)*, ser. Lecture Notes in Computer Science, vol. 11964, 2019, pp. 64–79.
- [51] F. Mirus, T. C. Stewart, and J. Conradt, "The Importance of Balanced Data Sets: Analyzing a Vehicle Trajectory Prediction Model based on Neural Networks and Distributed Representations," in *International Joint Conference on Neural Networks (IJCNN)*, 2020, pp. 1–8.
- [52] K. Shridhar, H. Jain, A. Agarwal, and D. Kleyko, "End to End Binarized Neural Networks for Text Classification," in *Workshop on Simple and Efficient Natural Language Processing (SustaiNLP)*, 2020, pp. 29–34.
- [53] D. Kleyko, E. P. Frady, M. Kheffache, and E. Osipov, "Integer Echo State Networks: Efficient Reservoir Computing for Digital Hardware," *IEEE Transactions on Neural Networks and Learning Systems*, vol. PP, no. 99, pp. 1–14, 2020.
- [54] E. P. Frady, D. Kleyko, and F. T. Sommer, "A Theory of Sequence Indexing and Working Memory in Recurrent Neural Networks," *Neural Computation*, vol. 30, pp. 1449–1513, 2018.
- [55] T. A. Plate, *Distributed Representations and Nested Compositional Structure*. University of Toronto, PhD Thesis, 1994.
- [56] V. I. Gritsenko, D. A. Rachkovskij, A. A. Frolov, R. W. Gayler, D. Kleyko, and E. Osipov, "Neural distributed autoassociative memories: A survey," *Cybernetics and Computer Engineering*, vol. 2, no. 188, pp. 5–35, 2017.
- [57] T. A. Plate, "Holographic Reduced Representations," *IEEE Transactions on Neural networks*, vol. 6, no. 3, pp. 623–641, 1995.
- [58] B. Komer, *Biologically Inspired Spatial Representation*. University of Waterloo, PhD Thesis, 2020.
- [59] A. Ultsch, "Clustering with SOM: U* C," in *Workshop on Self-Organizing Maps*, 2005.
- [60] U. Quasto, M. Richter, and C. Biemann, "Corpus Portal for Search in Monolingual Corpora," in *Fifth International Conference on Language Resources and Evaluation (LREC)*, 2006, pp. 1799–1802.
- [61] A. Rahimi, P. Kanerva, and J. Rabaey, "A Robust and Energy Efficient Classifier Using Brain-Inspired Hyperdimensional Computing," in *IEEE/ACM International Symposium on Low Power Electronics and Design (ISLPED)*, 2016, pp. 64–69.
- [62] A. Joshi, J. Halseth, and P. Kanerva, "Language Geometry Using Random Indexing," in *Quantum Interaction (QI)*, 2016, pp. 265–274.
- [63] E. P. Frady, G. Orchard, D. Florey, N. Imam, R. Liu, J. Mishra, J. Tse, A. Wild, F. T. Sommer, and M. Davies, "Neuromorphic nearest neighbor search using intel's pohoiki springs," in *Neuro-Inspired Computational Elements Workshop (NICE)*, 2020.
- [64] M. Zeman, E. Osipov, and Z. Bosnic, "Compressed Superposition of Neural Networks for Deep Learning in Edge Computing," in *International Joint Conference on Neural Networks (IJCNN)*, 2021, pp. 1–8.
- [65] P. Kanerva, *Sparse Distributed Memory*. The MIT Press, 1988.